

Measurement of the Proton Elastic Form Factor Ratio at Low Q^2

J. Arrington (spokesperson), K. Hafidi, R. Holt, D. Geesman, P. Reimer,
and P. Solvignon

Argonne National Laboratory, Argonne, IL, USA

R. Gilman (spokesperson), X. Jiang, E. Kuchina, G. Kumbartzki,
R. Ransome, and E. Schulte

Rutgers, The State University of New Jersey, Piscataway, New Jersey 08854, USA

J. Glister and A. Sarty (spokesperson)

St. Mary's University, Halifax, Nova Scotia, B3H C3C Canada

J. Lichtenstadt, E. Piasetzky, I. Pomerantz, G. Ron (spokesperson)¹, and
R. Shneur

Tel Aviv University, Tel Aviv, 69978 Israel

A. Camsonne, J.P. Chen, E. Chudakov, J.-O. Hansen,
D.W. Higinbotham (spokesperson), C.W. de Jager, M. Jones,
J.J. LeRose, D. Meekins, A. Saha, and V. Sulkosky

Thomas Jefferson National Accelerator Facility, Newport News, VA 23606, USA

D. Day (spokesperson), R. Lindgren, B.E. Norum, K. Paschke, K. Slifer,
K. Wang, and X. Zheng,

University of Virginia, Charlottesville, VA 22904, USA

F. Sabatie

CEN Saclay, 91191 Gif-Sur-Yvette Cedex, France

E. Brash

Christopher Newport University, Newport News, VA, USA

D. Armstrong, T. Averett, L. Pentchev, and C.F. Perdrisat

College of William & Mary, Williamsburg, VA, USA

W. Chen, H. Gao, X. Qian, and X. Zhu

Duke University, Durham, NC, USA

P. Markowitz and W. Boeglin

Florida International University, Miami, FL, USA

L. Bimbot

Institut de Physique Nuclaire d'Orsay, BP n1, F91406, Orsay Cedex, France

B. Anderson

Kent State University, Kent, Ohio 44242, USA

W. Bertozzi, S. Gilad, J. Huang, B. Moffit, A. Puckett, and X. Zhan

Massachusetts Institute of Technology, Cambridge, MA 02139, USA

V. Punjabi

Norfolk State University, Norfolk, VA, USA

A. Beck and S. Maytal-Beck

Nuclear Research Center Negev, P.O.Box 9001, Beer-Sheva, Israel

L. Weinstein

Old Dominion University, Norfolk, VA, USA

K. McCormick

Pacific Northwest National Lab, Richland, WA, USA

T. Holmstrom

Randolph-Macon College, Ashland, VA, USA

Seonho Choi, Ho-young Kang, Hyekoo Kang, Byungwuek Lee,
Yoomin Oh, and Jeongseog Song

Seoul National University, Seoul 151-747, Korea

B. Sawatzky

Temple University, Philadelphia, PA, USA

C. Muñoz Camacho

Université Blaise Pascal/CNRS-IN2P3, F-63177 Aubière, France

J. Annand, D. Hamilton, D. Ireland, D. Protopopescu, and G. Rosner

University of Glasgow, Glasgow, G12 8QQ, Scotland, UK

M. Mihovilovič, M. Potokar and S. Širca

Jožef Stefan Institute and University of Ljubljana, Ljubljana, Slovenia

F. Benmokhtar

University of Maryland, College Park, MD, USA

J. Calarco

University of New Hampshire, Durham, NH, USA

G. Huber

University of Regina, Regina, SK S4S0A2, Canada

S. Strauch

University of South Carolina, Columbia, SC, USA

and

The Hall-A Collaboration

Abstract

We propose to study the proton elastic form factor ratio $\mu G_E/G_M$ in the range of $Q^2 = 0.01 - 0.7 \text{ GeV}^2$. Our goal is to vastly improve the knowledge of the ratio at low Q^2 , which, in combination with separate cross section data, will also allow significant improvements in knowledge of the individual form factors. In this low Q^2 range, substantial deviations of the ratio from unity have been observed, and data, along with many fits and calculations, continue to suggest that structures might be present in the individual form factors, and in the ratio. Beyond the intrinsic interest in the structure of the nucleon, improved form factor measurements also have implications for deeply virtual Compton scattering, for determinations of the proton Zemach radius, and for parity violation experiments. The experiment has two parts which necessarily must run separately. We request 14 days in Hall A with 80% polarized beam to make recoil polarimetry measurements with the FPP for the higher Q^2 data ($0.25 \text{ GeV}^2 < Q^2 < 0.7 \text{ GeV}^2$). We request 11 days in Hall A with 80% polarized beam to make polarized beam – polarized target asymmetry measurements, with the UVa NH_3 target and the septum ($0.015 \text{ GeV}^2 < Q^2 < 0.4 \text{ GeV}^2$). The total time request is for 25 days in Hall A with 80% polarized beam. The recoil polarimetry measurements were conditionally approved by PAC31, here we propose an additional set of measurements (an incremental increase of 11 days) which will extend the approved range of measurements a factor of 20 lower in Q^2 .

¹ contact person: Guy Ron, gron@jlab.org

Background

Since the proton magnetic moment differs from that of a structureless Dirac particle

$$\mu \neq \frac{q}{mc} |\vec{s}|, \quad (1)$$

where μ , q , m , and s are the magnetic moment, electric charge, mass and spin of the particle, respectively, and c is the speed of light, these particles must have an internal structure. Electron scattering experiments were used starting in the 1950s to unravel the distributions of electric charge and magnetization in the nucleons. The elastic scattering cross section is given by a product of the scattering cross section from a point-like particle, multiplied by form factors that contain the information about the internal structure of the nucleons:

$$\frac{d\sigma}{d\Omega} = \frac{\alpha^2}{Q^2} \left(\frac{E'}{E} \right)^2 \frac{\cot^2 \frac{\theta_e}{2}}{1 + \tau} \left[G_E^2 + \tau \left(1 + 2(1 + \tau) \tan^2 \frac{\theta_e}{2} \right) G_M^2 \right] = \sigma_{Mott} \left[G_E^2 + \frac{\tau}{\varepsilon} G_M^2 \right] \quad (2)$$

Here α is the electromagnetic coupling constant, Q^2 is the four-momentum transfer, E and E' are the electron incoming and outgoing energies, θ_e is the electron scattering angle, $\tau = Q^2/4m_p$, and G_E and G_M , which depend on Q^2 , are the electric and magnetic form factors, σ_{Mott} is the Mott cross section for electron scattering from a point-like particle and ε is the virtual photon polarization. The form factors have usually been determined with a ‘‘Rosenbluth Separation’’ [1], in which the eN elastic cross section is measured at different beam energies and angles, corresponding to different ε values but the same momentum transfer. In non-relativistic quantum mechanics, the charge and magnetization spacial distributions are connected to the form factors through a Fourier transform; in relativistic quantum mechanics, understanding the spacial distributions is problematic, as they are model dependent.

The nucleon form factors (except for G_E^n which must go to zero as $Q^2 \rightarrow 0$) were found to approximately follow the **dipole form factor** formula,

$$G_D = \left(1 + \frac{Q^2}{\lambda_D^2} \right)^{-2},$$

where $\lambda_D^2 \approx 0.71 \text{ GeV}^2$ is an empirical parameter found to be identical for the three form factors G_E^p , G_M^p , and G_M^n , so that $G_E^p \approx G_D$, and $G_M^{p,n} \approx \mu_{p,n} G_D$. The dipole form factor corresponds to an exponential charge and magnetization distribution, which would result from a δ -function potential. In so far as the nucleon is small, this observation makes some intuitive sense. Since in the dipole approximation all form factors are equal except for an overall scale, it is evident that the ratio of the proton electric to magnetic form factors (multiplied by the proton magnetic moment) should be equal to one.

Starting in the late 1960’s and early 1970’s, experiments started to observe deviations from the simple dipole formulas for the form factors. For example, Bartel *et al.* [2] and Berger *et*

al. [3] observed deviations at the level of a few tens of percent at high Q^2 , 1 GeV² or so, for G_E^p and G_M^p . But these measurements were not very precise, and more precise recent cross section measurements from SLAC [4,5] and Jefferson Lab [6,7] indicate better agreement, to within about 10%, with the dipole formula at high Q^2 . Some of the recent data, for the form factor ratio, are shown in Figure 1, taken from [7]. In the 1970's and 1980's, more precise cross section measurements on the proton [8–10] at low Q^2 also observed deviations from the dipole formulas of a few percent at low Q^2 , but these observations appear to have had little impact, with interest in form factors largely focused on high Q^2 and G_E^n .

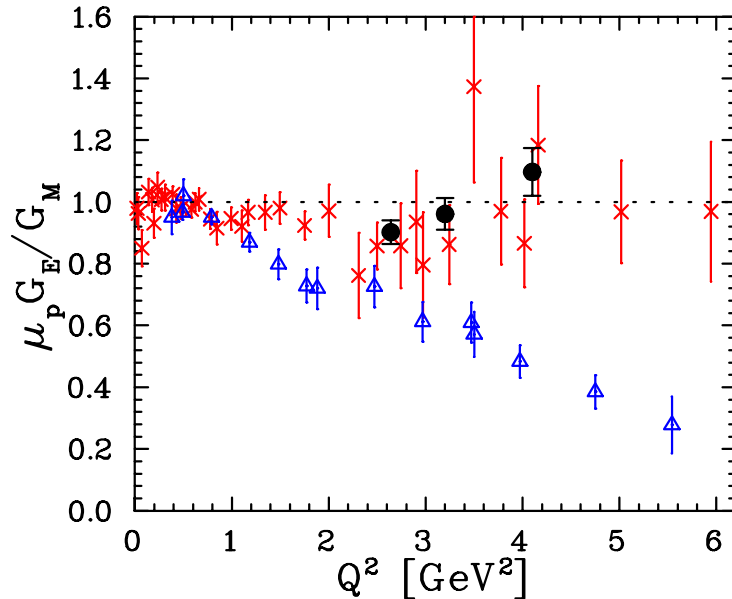


Fig. 1. Data on the proton Electric to Magnetic Form Factor Ratio, including the older Rosenbluth separation data (crosses) from a global reanalysis [11], newer polarization transfer data [12–14] (triangles) and the most recent JLab Rosenbluth separation data [7] (filled circles).

Starting before there were any quark models for the nucleon structure, and continuing to this day, theory and many fits for the form factors have often used a vector-meson-dominance (VMD) picture, in which a photon couples to a proton through virtual quark–anti-quark states, the vector mesons [15–23]. In the VMD picture, the observed dipole form factor is simply a good approximation to a sum of monopoles that represent vector meson exchanges. The best such fits typically use several monopoles with masses that do not correspond to physical meson masses. More recent quark-model calculations include such approaches as constituent quarks, a quark core surrounded by a pion cloud, or a chiral quark model [24–29].

For the past decade, most new form factor measurements have relied on polarization techniques. The *Recoil Polarization* method [30–32] has been used by most recent measurements [12–14,33,34] to extract the proton form factor ratio, whereas polarized beam – polarized target asymmetries have been more common for neutron form factor measurements. The proton form factor ratio is calculated from the ratio of transferred polarization

components of the recoil proton:

$$\frac{G_E}{G_M} = -\frac{P_x E + E'}{P_z 2M_p} \tan \frac{\theta_e}{2}. \quad (3)$$

Here P_x and P_z are the transferred polarization components,

$$\sigma_{red} P_x = -2\sqrt{\tau(1+\tau)} \tan \frac{\theta_e}{2} G_E G_M, \quad \text{and} \quad (4)$$

$$\sigma_{red} P_z = \frac{E + E'}{M_p} \sqrt{\tau(1+\tau)} \tan^2 \frac{\theta_e}{2} G_M^2. \quad (5)$$

where σ_{red} is the reduced cross section.

The recoil polarization form factor measurements show a strong deviation at high Q^2 from the expected ratio of one [12,14,34]; see Figure 1. It is now generally accepted theoretically that two-photon exchange corrections account for much, if not all, of the differences between the Rosenbluth and polarization transfer techniques – see [35–39]. It is believed that these corrections have little impact on the polarization technique for determining form factors, but have large impact on the Rosenbluth technique, as both two-photon corrections and the electric form factor typically contribute a few percent of the cross section at high Q^2 . Such corrections have been cleanly demonstrated in low Q^2 transverse beam asymmetries in parity-violation measurements [40,41], but not in high Q^2 form factor measurements; several such experiments have been approved by the Jefferson Lab PAC and are awaiting beam time.

Recent measurements in Hall A [42] have demonstrated the recoil polarization method to be effective at low Q^2 , however, these measurements were taken in a short time with low beam polarization. Since the systematic uncertainties for this measurement are small it is trivial to perform a higher precision measurement using the recoil polarization method, down to about $Q^2 \approx 0.3 \text{ GeV}^2$. Despite the above, the recoil polarization method has some drawbacks when considering a very low Q^2 measurement. First, the method of recoil polarization relies on a secondary scattering which takes place in a (usually) carbon analyzer. When performing a low- Q^2 measurements, the recoil proton is ejected with too low a momentum to be detected in the rear drift chambers. Second, due to the low energy of the ejected proton it loses a significant fraction of its momentum in traversing the target cell, rendering an accurate measurement difficult owing to the need to take into account the energy loss due to multiple scattering. And last, the energy of the recoil proton favors an elastic secondary scattering with the carbon nuclei in the analyzer, a process resulting in a larger analyzing power for large scattering angles, resulting in a reduction of the figure of merit of the polarimeter in the acceptance range of the Hall A FPP.

Thus, we further suggest to use an alternative method to measure the form factor ratio to much lower Q^2 values, using a double-spin-asymmetry (**DSA**) measurement of the reaction $\vec{p}(\vec{e}, e')p$, using a simultaneous measurement with two spectrometers. This method has been proposed before in PR-01-105 [43] as a cross check on the recoil polarization

method, in the Q^2 range where significant disagreement was found with the Rosenbluth data. The previous proposal was deferred due to a lack of compelling reason to perform the measurement at the proposed data points ($Q^2 = 1.1, 2.1 \text{ GeV}^2$)². This proposal, while proposing the same method to measure the form factor ratio, suggests a much lower Q^2 range which will not only provide an extremely high precision cross check, but also significantly improve the knowledge of the form factors at very low Q^2 values. This is particularly important for G_M^P , for which the cross section is largely insensitive at low Q^2 , except for a very limited range of measurements near 180° .

Motivation

While interest in the low Q^2 form factors languished for a while, these studies have recently become much more compelling. First, the form factors are fundamental properties of the nucleon that should be measured well to test our understanding of the nucleon; as we shall demonstrate in this proposal, it is now possible to measure the form factors with a large improvement in the uncertainties. Second, although theory generally indicates the form factors have smooth shapes as one varies Q^2 , there are an unsatisfyingly large number of theory calculations, fits, and data points that suggests this might not be the case – that there might be narrow structures in the form factors. The proposed measurement is good enough to either confirm or refute all existing suggestions of few percent structures in the form factors, or in the form factor ratio. Third, it has become apparent that the existing uncertainties in the form factors are among the leading contributions to uncertainties in determining other physics quantities, such as the nucleon Zemach radius, the strange form factors determined in parity violation, and the generalized parton distributions determined in deep virtual Compton scattering. The improvement possible with the proposed measurements is substantial.

Interest in the low Q^2 proton form factors was reinvigorated by the possibility of structures in the form factors. Most notably, an analysis by Friedrich and Walcher [44] fit all the nucleon form factors, finding deviations in the fits that indicate structures at low Q^2 , which they interpret as evidence of the virtual pion cloud surrounding the nucleon.³ Using both a phenomenological fit and a fit based on the constituent quark model, the authors have shown that it is possible to fit all four nucleon form factors coherently with both ansatzes and that all four show the signal of the pion cloud. However, other modern form factor fits find no need for additional narrow structures. These previous examinations of pion cloud contribution have mainly looked at the structure relative to the dipole form (except for G_E^N). The proposed measurement, will for the first time, allow for a precise model–

² The PAC report on PR-01-105 may be found in Appendix A

³ The nucleon form factors have of course been fit with various functional forms. One should not be too surprised if the form factors do not happen to follow some particular parameterization. Furthermore, one should be concerned about whether deviations from a particular functional form represent new physics, as opposed to an inappropriate parameterization.

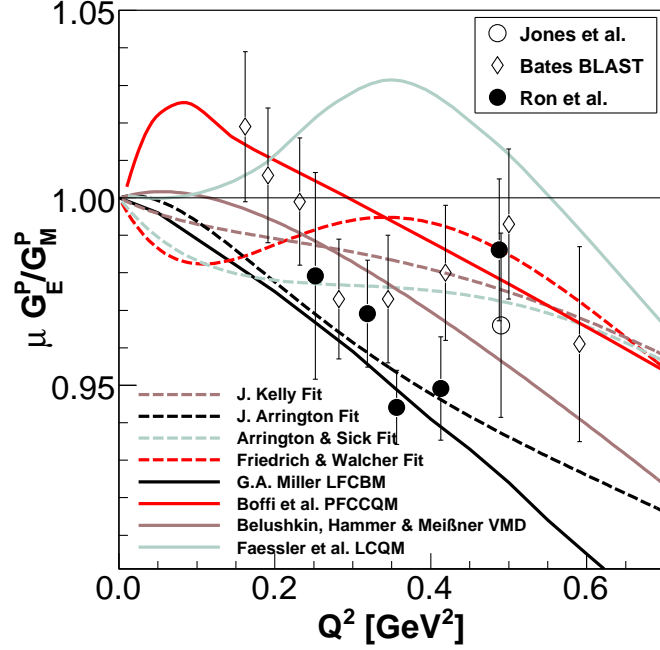


Fig. 2. High-precision results for the proton form factor ratio, compared to several fits and parameterizations.

independent comparison of the behavior of G_M^P and G_E^P , which does not depend on the dipole form being appropriate at low Q^2 .

The situation for the proton form factor ratio is depicted in Figure 2. The ratio was measured to about 2% by the Bates BLAST experiment. Our recent “LEDEX” data has uncertainties as small as nearly 1%. The data show that the ratio clearly drops below unity by $Q^2 = 0.3 \text{ GeV}^2$. While the data are consistent with a smooth falloff of the ratio above about 0.2 GeV^2 , similar to the Belushkin *et al.* curve, they also (“perhaps unfortunately”) suggest a potential structure at $Q^2 \approx 0.3 \text{ GeV}^2$. The solid lines are three different quark model calculations. Note that both the Boffi *et al.* [27] and Faessler *et al.* [28] calculations show structures in the ratio, but they tend to be higher than the data. Nevertheless, they suggest that narrow structures might be theoretically possible. From the recent fits and data shown, one can conclude that the ratio is only known to within about $\pm 2\%$ over much of the low Q^2 range. Of particular note is the fit by Friedrich and Walcher, which crosses over the data near $Q^2 = 0.25 \text{ GeV}^2$, indicating that the structures found in that fit are not actually present.

By combining the polarization data with previous cross-section results, it is possible to extract the individual form factors. Figure 3 shows the individual form factors as a function of ε at $Q^2 = 0.389 \text{ GeV}^2$, together with the calculated form factors using the same fits and calculations and color codes shown in Fig. 2. These are obtained by combining the highest precision existing cross-section data in the vicinity of the measured ratio [3] with the average of our form-factor ratios from $Q^2 = 0.36 \text{ GeV}^2$ and 0.41 GeV^2 . The figure shows that the form-factor extraction is essentially independent of ε , the virtual

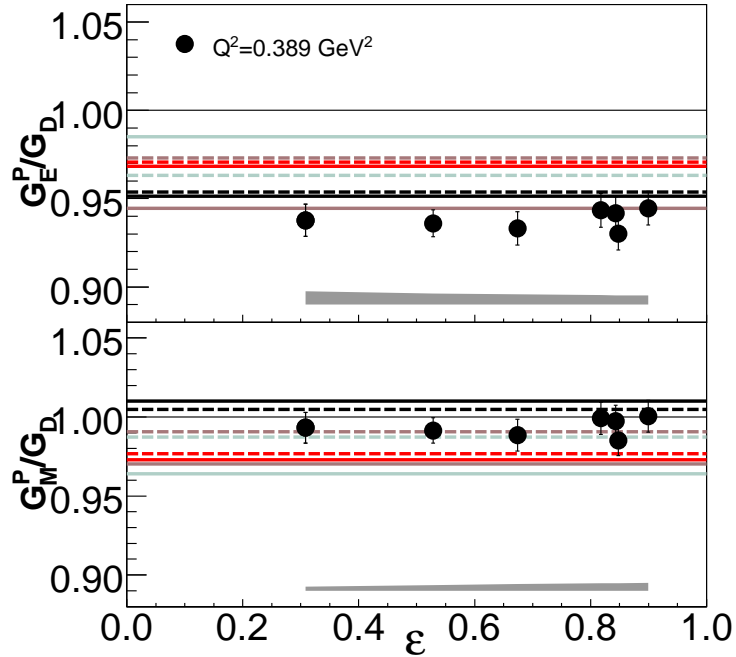


Fig. 3. The electric and magnetic form factors extracted from the polarization data and the individual cross sections of Berger *et al.*

photon polarization, over the extracted range. The deviation from unity in the ratio is dominated by the electric form factor. This result is consistent with previous Rosenbluth separation measurements and fits in this region of Q^2 ; the Rosenbluth results tend to have $\sim 1\text{--}3\%$ uncertainties for each of the form factors, while the fits vary by several percent for each [11]. While the Belushkin *et al.* fit [23] is generally best over the low Q^2 range, and at $Q^2 = 0.389 \text{ GeV}^2$ it is closest to G_E^p , it over predicts $R \equiv \mu_P G_E^p / G_M^p$ by underestimating G_M^p . The best fit of the ratio at $Q^2 = 0.389 \text{ GeV}^2$ is from Arrington [11], which over predicts each form factor by about 2%. The best calculations shown of the ratio at $Q^2 = 0.389 \text{ GeV}^2$ are from Cardarelli *et al.* [24] and Miller [26,45]. The Miller calculation over predicts each form factor by about 1-2%. Although the ratio is well reproduced by the Cardarelli *et al.* calculation, the individual form factors (not shown in Fig. 3) are significantly overestimated by the small-sized wave functions generated by present quark potential models [46].

Figure 4 shows how the knowledge of the form factor ratio at low Q^2 will be improved by the current proposal. Existing fits, calculations, and data are shown in the bottom part of the figure, similar to Figure 2. In the upper part of the figure, the gray bands represent the expected error band from the Mainz cross sections measurements underway [47]. This band arises from assuming the ratio is extracted by doing a Rosenbluth separation, neglecting two-photon corrections, and assuming the experiment achieves its ambitious planned 1% absolute uncertainty in the cross section measurements, the outer band represents the same calculation for a more realistic 1.5% uncertainty on the cross section measurements. The uncertainty grows at low Q^2 primarily because the beam energy can-

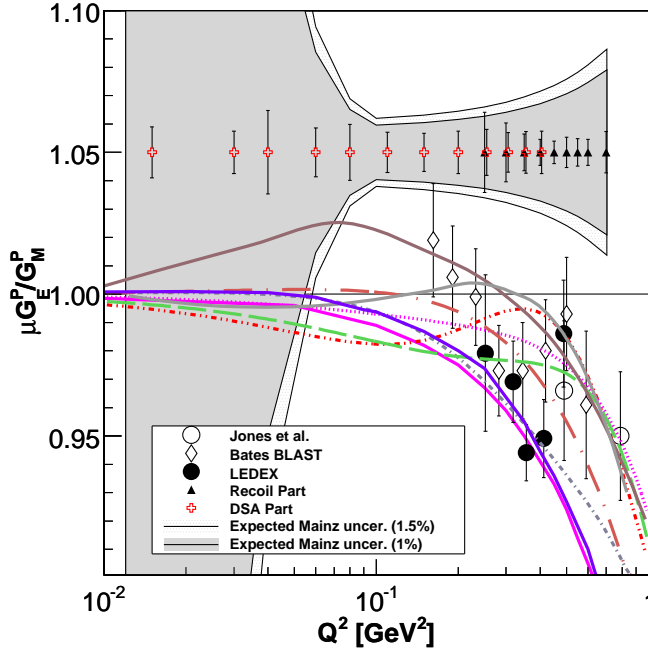


Fig. 4. Polarization transfer as a function of Q^2 . The data and curves in the lower part of the figure are the same as shown earlier. The gray bands represents the expected results from the Mainz cross section measurement (for both 1% and 1.5% cross section uncertainties). The data points set within the gray band represent the expected results of this proposal, from FPP measurements in black, and from polarized target asymmetries in red. The lowest point of the recoil polarization measurements will not be taken if both parts of the experiment are approved.

not be set low enough to reach small ε at low Q^2 , increasing the uncertainty on G_M (for an overview of the accessible range of ε vs. Q in the Mainz experiment see Fig. 5). For a small range of Q^2 near $0.1 - 0.2 \text{ GeV}^2$, Mainz can cover a large fraction of the ε range. At higher Q^2 , the high ε region cannot be reached, so the uncertainty on G_E and the ratio increase. Within the gray band, the data points shown indicate the expected results of this proposal. The black points in the higher Q^2 range shown are the anticipated results using the recoil polarimetry technique, while the red points at lower Q^2 are the results using polarized target asymmetries. It can be seen that our expected results are about 0.5 – 1% determinations of the form factors, leading to significant improvements at all Q^2 , ranging from about a factor of two near 0.2 GeV^2 , to much greater improvements near the ends of the Q^2 range. Note, that current data sets show a deviation from scaling at $Q^2 > 0.3 - 0.5 \text{ GeV}^2$, however, all calculations (solid lines) predict deviations from scaling at $Q^2 < 0.5 \text{ GeV}^2$. This measurement will have the necessary precision to provide a meaningful test of these calculations.

The improvements in the individual form factors are shown in Figures 6 and 7. As indicated above, the large-angle, low- ε Mainz cross section points dominate the determination of G_M , except where these points cannot be reached at the lowest Q^2 , so over much of the Q^2 range there is not an improvement in the magnetic form factor. In contrast, there

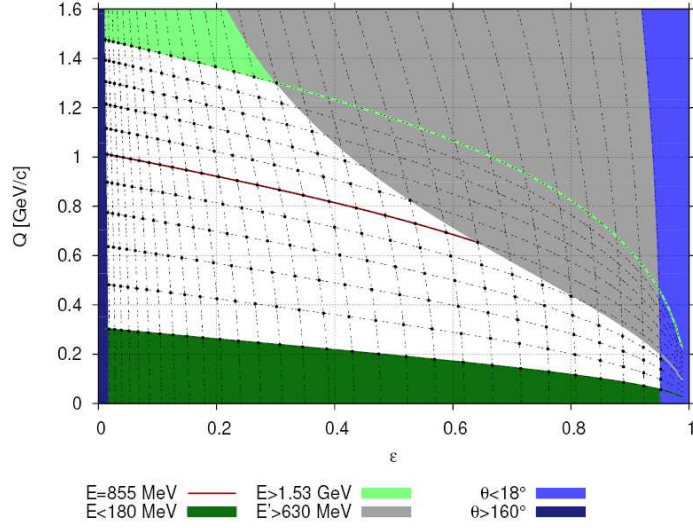


Fig. 5. The accessible kinematics for the Mainz measurement. Measurements are indicated by the white region of the plot. The dots indicate the points at which the spectrometers will be centered for taking data.

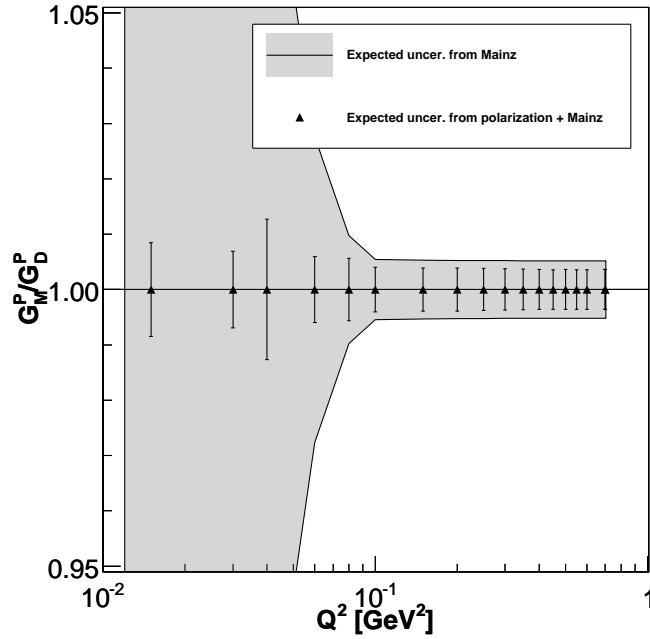


Fig. 6. Projected uncertainties on the extraction of G_M^P from a combination of this proposal and the Mainz cross section data, vs. the expected uncertainties from the Mainz extraction alone. Assuming a 1% uncertainty on the cross sections.

is significant improvement in the electric form factor at nearly all Q^2 , except for a small region near 0.1 GeV^2 . Note that Figs. 6 and 7 assume the optimistic 1% uncertainty on the cross sections.

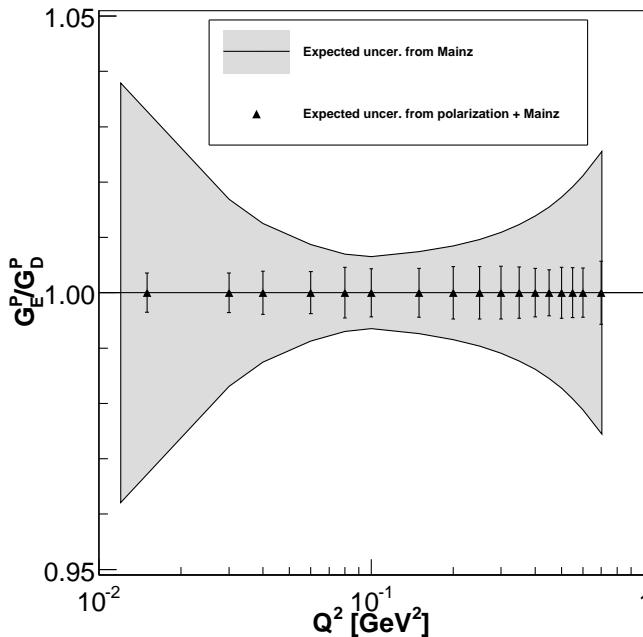


Fig. 7. Projected uncertainties on the extraction of G_E^P from a combination of this proposal and the Mainz cross section data, vs. the expected uncertainties from the Mainz extraction alone. Assuming a 1% uncertainty on the cross sections.

Summary of the proposed measurements

For the form factor ratio, we can provide an independent superior measurement, compared to Mainz. The 2 – 3% structures hinted at by the high precision form factor ratio data can be definitively ruled out or confirmed by our 0.5 – 1% proposed measurements – at present we believe that the data are consistent enough with the Belushkin *et al.* curve that one cannot claim any structures exist.

For the individual electric and magnetic form factors, the use of our form factor ratio data along with the Mainz cross section data provides a precise check that the individual form factors are independent of ε , an important check of two-photon effects – which are expected to be at the few tenths of a percent level from calculations – and of experimental systematics. The resulting determination of G_M is a semi-independent check at the same level of uncertainty as using only the cross section measurements. The resulting determination of G_E is a semi-independent superior determination of the electric form factor.

Recent theoretical work

A recent theoretical calculation by Miller [48] enhances the motivation for better low Q^2 form factor determinations.

Miller has found basically that the difference between the electric and magnetic radii – what one would measure if one could determine the rest-frame distributions – requires a correction to the observed slope in the form factors that corresponds to the anomalous magnetic moment, and essentially all data and fits lead to a true magnetic radius that is larger than the electric radius. However, the size of this difference is highly uncertain, and can be much improved by improved form factor determinations. Figure 8 shows the difference between the true magnetic and electric radii as calculated by Miller *et. al.* for different fits, theoretical calculations and for the world dataset for low Q^2 ratio measurements together with the projected uncertainty from this proposal.

The method proposed by Miller *et al.* requires a fit to the form factor ratio at low Q^2 where the ratio is assumed to be linear with Q^2 . Current world data do not allow do determine the linearity of the ratio at low Q^2 leading to an uncertainty on $R_E^{*2} - R_M^{*2}$ (where R_E^{*2} and R_M^{*2} are the *effective radii* of [48]) of approximately 50%. While the existing fit to the world data appears to contradict several of the fits and calculations, there is an inherent uncertainty since it is not clear that the fit covers only the linear region. The new data will dramatically improve the uncertainties while providing a much clearer indication of whether the data follow a linear behavior.

Impact on Other Measurements

We now indicate how the greater precision will impact other processes, such as determining the nucleon Zemach radius, the strange form factors from parity violation, and the generalized parton distributions from deep virtual Compton scattering. The improvement possible with the proposed measurements is substantial.

The proton Zemach radius [49] is given by

$$r_z = -\frac{4}{\pi} \int_0^\infty \frac{dQ}{Q^2} \left[\frac{G_E(Q^2)G_M(Q^2)}{(1 + \kappa_p)} - 1 \right]. \quad (6)$$

It is of particular interest in understanding the hyperfine splitting in hydrogen. It is evident that the Zemach radius is most sensitive to the form factors at low Q^2 . It is pointed out in [49] that differences between modern form factor parameterizations lead to about 0.6 ppm changes in estimates of the Zemach radius correction to the theory; since the theory is at about the 1 ppm level, the form factor uncertainties are then among the leading uncertainties in the theoretical prediction. Thus, efforts to improve the knowledge of the form factors are important to improving the theoretical uncertainties.

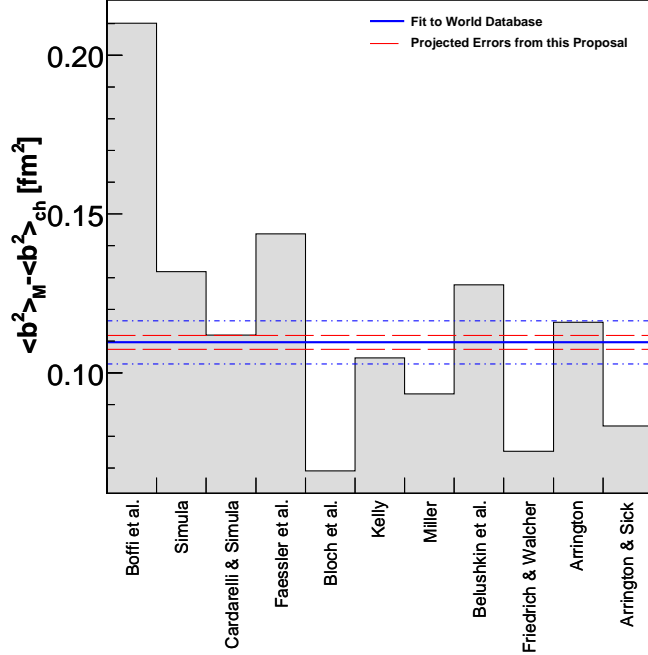


Fig. 8. $\langle b^2 \rangle_m - \langle b^2 \rangle_{ch}$ from recent calculations and fits. All the fits and calculations yield a positive value. The blue lines are from the fit to the world data set and the dashed red lines are the projected uncertainties from this proposal ($\langle b^2 \rangle_{m(ch)}$ are defined in [48]).

Our own understanding, given for example the results shown in Figure 3, is that this result is optimistic about the actual uncertainties in the form factors at low Q^2 , and the calculated Zemach radius could be off by around 2% or about 1 ppm. There is a similarly sized contribution to the integral from the high- Q^2 region, where G_E is unknown and might actually change sign; this region will be better understood from the G_E^p -III experiment and future 12-GeV work.

The improved knowledge of the form factors can also have a significant effect on the strange form factors determined in parity violation experiments. For example, for the HAPPEX measurement of the weak form factors [50] the new data adjust the measured asymmetry by about -0.5 ppm, corresponding to a smaller effect from strange quarks, on data with a statistical uncertainty of ≈ 1 ppm. If there is a similar effect on the G0 results, which have similar kinematics and uncertainties, than improved measurements of the form facts would have implications for the extraction of strange form factors in G0. Finally, our published measurement implies a shift in the expected HAPPEX-III result [51] by one standard deviation. It should be clear that the new proposed measurements can have significant effects on the determination of the strange form factors for the parity violation measurements.

For Deep Virtual Compton Scattering, which is used to access generalized parton distributions, the process depends on knowledge of the form factors at low $Q^2 = -t$ - the form factors are evaluated at a four momentum corresponding to the small difference in

virtual and real photon momenta, rather than the large virtual photon four-momentum. In general these experiments appear to assume that one can calculate the Bethe-Heitler contribution from the form factors to 1%, based on a comparison of form factor fits. Our understanding, as indicated above, is that this is optimistic. However, at this point the precision of the measurements is such that the uncertainty in the Bethe-Heitler contribution is not a leading uncertainty.

Part I: Recoil Polarization Measurement

Overview of Technique

This proposed experiment follows directly on previous Hall A form factor ratio measurements. As compared to our recent low Q^2 data [42], we improve the uncertainties by a factor of about 3 by requiring a beam polarization of 80%, instead of 40%, and by running each point for approximately twice as long.

An overview of the experimental setup is shown in Fig. 9. We use both HRSs in the standard configuration to perform a coincidence measurement of the scattered proton and electron, to reduce potential backgrounds. The polarization of protons exiting the target is determined by the focal plane polarimeter (FPP) in the left HRS.

Observables

We plan to measure:

- $P_{x'}$: The transferred polarization component in the scattering plane perpendicular to the proton momentum.
- $P_{z'}$: the transferred polarization component in the scattering plane parallel to the proton momentum.

We extract the proton form factor ratio $\mu \frac{G_E}{G_M}$ from the polarization transfer measurements:

$$R \equiv \mu_p \frac{G_E}{G_M} = -\mu_p \frac{P_x E + E'}{P_z 2M_p} \tan \frac{\theta_e}{2}. \quad (7)$$

FPP

The experiment measures the polarization of low to medium energy protons, with momenta from 0.5 – 1 GeV/c. We plan to use the thinner carbon analyzers of the Hall A

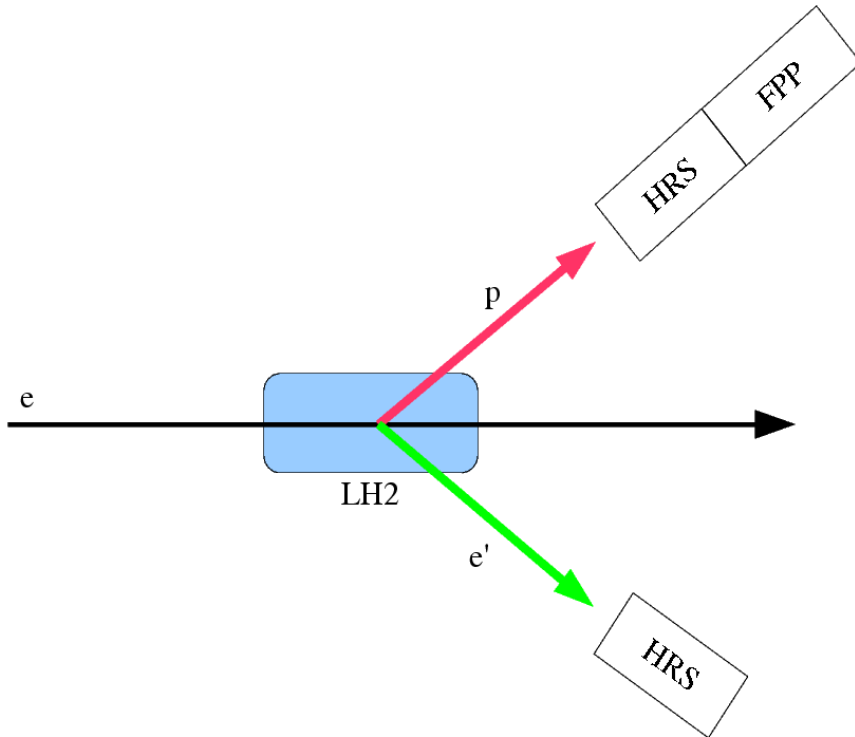


Fig. 9. Experimental Setup for part I of the Proposed Experiment.

FPP, basing our choice of analyzer on the previous measurements done during the the LEDEX experiments [52,53]. The analyzing power in these kinematics is large, and is a well known function of the proton energy, from both the McNaughton parameterization [54] and the measured analyzing power of our previous low energy experiment [55].

The polarization transfer from longitudinally-polarized electrons gives the protons an in-plane polarization. The form factor ratio is basically determined from the orientation of this in-plane polarization, while the product of the beam helicity and FPP analyzing power is determined from its magnitude. Thus, the form factor ratio can be determined without knowing the analyzing power or the beam polarization; still, if these are large, the asymmetry directly measured by the FPP is larger, and thus the direction of the polarization vector is determined with smaller uncertainties.

The level of the achievable systematics in this kinematic range was studied in the most detail in the first Hall A G_E^p experiment [34]. The systematic uncertainty on the form factor ratio was 0.4% at $Q^2 = 0.5 \text{ GeV}^2$, increasing to 1% at $Q^2 = 0.8 \text{ GeV}^2$. The systematic uncertainty is dominated by how well one can determine the spin direction at the target, from the spin direction measured in the spectrometer focal plane. The direction is changed by spin precession in the spectrometer magnets, and thus the uncertainties arise from the limited knowledge of the optics matrix elements of the spectrometer. The optics were tested both by studying distributions in the focal plane with, for example, quadrupoles

turned off, and by measuring ep elastic scattering at $Q^2 = 2.2 \text{ GeV}^2$. At this high Q^2 , the spin precession is near 180° , and the spin in the focal plane changes sign across the acceptance; thus one has high sensitivity to the spectrometer model.

The reason for the decrease in systematic uncertainty at $Q^2 = 0.5 \text{ GeV}^2$, and indeed for our entire experiment, is that spin precession is nearly optimal (for this experiment), with spin precession near 90° . Thus small differences in the bend angle make almost no difference in the form factor ratio. There is no reason to expect the systematic precision during this experiment will be significantly different from that achieved previously.

To check the experimental systematics, we always run each Q^2 point at multiple proton-arm momentum settings, so that we can see at what level the polarization is independent of the proton position in the focal plane. We also plan to do a limited series of optics measurements similar to those done for [34]; the central part of these measurements will be a measurement of ep elastic scattering at $Q^2 \approx 2.2 \text{ GeV}^2$, for the reasons discussed above.⁴ The statistical precision that we propose roughly matches the expected systematic precision.

Background

Because the low Q^2 ep coincidence cross sections are large, background rates are relatively small and backgrounds tend to be unimportant. The cosmic ray rate is negligible. Coincidence background events from the target end caps are suppressed due to Fermi motion – only a small fraction of the coincident ($e, e'p$) protons actually are within the spectrometer acceptance; reconstructed target position cuts remove any remaining background. Thus our expected signal rate is about our DAQ rate, which is about 2 – 2.5 KHz, of which a negligible fraction is removed by the target position cuts [42].

Kinematics and Time Request for Part I

The proposed kinematics are shown in Table 1.

While all of the data can be obtained with 1-pass beam, the $Q^2 = 2.2 \text{ GeV}^2$ measurement that tests the spin transport is optimally run at $E_e \approx 3.2 \text{ GeV}$; it requires one day. It can be run if needed at 2.4 or 4.0 GeV, but it would require an extra day to make up for the decrease in coincidence efficiency due to the mismatch in the spectrometers.

Since we aim to take high statistics data and do not require a low dead time, our plan is to run with data rates of about 2 – 3 KHz, as we did during E05-103. These rates

⁴ Note that the previous studies were done with the FPP in HRS-right; the FPP is now in HRS-left.

Table 1
Proposed Kinematics

Beam Energy [GeV]	Q^2 [GeV ²]	θ_e [deg]	E' [GeV]	θ_p [deg]	P_p [GeV/c]
0.845	0.25	37.611	0.711	57.088	0.517
0.845	0.30	42.191	0.685	53.751	0.570
0.845	0.35	46.726	0.659	50.614	0.620
0.845	0.40	51.288	0.632	47.622	0.667
0.845	0.45	55.942	0.605	44.734	0.712
0.845	0.50	60.750	0.578	41.915	0.756
0.845	0.55	65.774	0.552	39.136	0.797
0.845	0.60	71.089	0.525	36.369	0.838
0.845	0.70	82.969	0.472	30.754	0.916
3.2	2.2	33.853	2.027	36.687	1.172

can be attained with beam currents from a few μA up to about $80 \mu\text{A}$, and with dead times of about 30%. Other experiments have run with higher dead times; it is not an issue for a recoil polarization experiment. We will use a standard 15 cm ($\approx 1.05 \text{ g/cm}^2$) liquid hydrogen target. Time estimates were made using these conditions and standard ep cross section calculations. Twenty-four hours at each kinematic setting – except 48 hours for the lowest Q^2 point – results in uncertainties of 1% or less – see Table 2 – for the form factor ratio, assuming a beam polarization of $\approx 80\%$. Then the statistical and systematic uncertainties are estimated to be approximately matched.

Table 2

Expected Uncertainties in the Form Factor Ratio Measurement (systematic uncertainties are assumed to roughly match the statistic uncertainties).

Q^2 [GeV ²]	$(\Delta \text{Ratio}/\text{Ratio})_{stat.}$ [%]	$(\Delta \text{Ratio}/\text{Ratio})_{total}$ [%]
0.25	1.00	1.41
0.3	0.73	1.03
0.35	0.46	0.65
0.4	0.32	0.45
0.45	0.28	0.39
0.5	0.37	0.52
0.55	0.34	0.48
0.6	0.32	0.45
0.7	0.31	0.43

Additional time is needed for the following purposes:

- 9 angle changes require 1 hour each.
- 20 spectrometer momentum changes require 30 minutes each.
- 1 straight through run is used to calibrate the FPP alignment. This requires about 1 hour.
- One beam energy change during the experiment, requiring about 8 hours.
- 10 pointing runs will be taken, totaling about 10 hours.
- Two Møller measurements of the beam polarization are needed, requiring about 8 hours.
- Systematic studies of the spin transport are needed to re-verify the results of the studies performed during the G_E^p -I measurement. We plan on about 1 day of measurements

using varying magnetic field settings, similar to the earlier studies.

With 10 days of data runs, plus ≈ 3 days of calibration and overhead, plus 1 day for the higher Q^2 measurement (systematic studies of spin transport at $Q^2 = 2.2 \text{ GeV}^2$), **our total time request for the recoil polarization part is for 14 days.**

If part II of the experiments is approved we plan to forgo the measurement of the lowest Q^2 (0.25 GeV^2) data point, since it is possible to measure this point with greater accuracy with the technique proposed for part II. This will reduce the beam time requested for this part to 12 days while still maintaining 3 extremely high precision overlap points in order to cross check the results.

Part II: Double Spin Asymmetry (DSA) Measurement

Overview of Technique

For elastic scattering of polarized electrons off polarized protons the cross section difference between helicity states is:

$$\frac{1}{2} [\sigma^+ - \sigma^-] = -2\sigma_{Mott} \frac{E'}{E} \sqrt{\frac{\tau}{1+\tau}} \tan \frac{\theta_e}{2} \left\{ \sqrt{\tau \left(1 + (1+\tau) \tan^2 \frac{\theta_e}{2} \right)} \cos \theta^* G_M^2 + \sin \theta^* \cos \phi^* G_M G_E \right\}. \quad (8)$$

Where θ_e , σ_{Mott} , E , E' are the same as in Eq. (2), and θ^* (ϕ^*) is the target spin polar (azimuthal) angle.

The asymmetry is then:

$$A \equiv \frac{\sigma_+ - \sigma_-}{(\sigma_+ + \sigma_-) P_b P_t f} = - \frac{2 \sqrt{\frac{\tau}{1+\tau}} \tan \frac{\theta}{2} \left\{ \sqrt{\tau \left(1 + (1+\tau) \tan^2 \frac{\theta}{2} \right)} \cos \theta^* G_M^2 + \sin \theta^* \cos \phi^* G_M G_E \right\}}{(P_b P_t f) \left(\frac{G_e^2 + \tau G_M^2}{1+\tau} + 2\tau G_M^2 \tan^2(\theta/2) \right)}, \quad (9)$$

where $P_b(P_t)$ are the beam (target) polarization and f is the dilution factor which reduces the amount of hydrogen seen by the beam due to the fact that the target, being composed of $^{15}\text{NH}_3$ also contains nitrogen atoms.

By measuring the asymmetry in HRS_{right} and HRS_{left} simultaneously **at the same value of Q^2** (i.e., the same spectrometer angle) we can take the ratio of the two measured asymmetries thus completely removing any systematic uncertainties resulting from the beam and target polarizations and the dilution factor. Note that since the two HRSs are identical, to first order $f_1 = f_2$, where f_1 and f_2 are the dilution factors for the first and second HRS, respectively.

Figure 10 shows the coordinate system for the reaction $\bar{p}(\vec{e}, e')p$. Figure 11 shows the kinematics for the two simultaneous measurements.

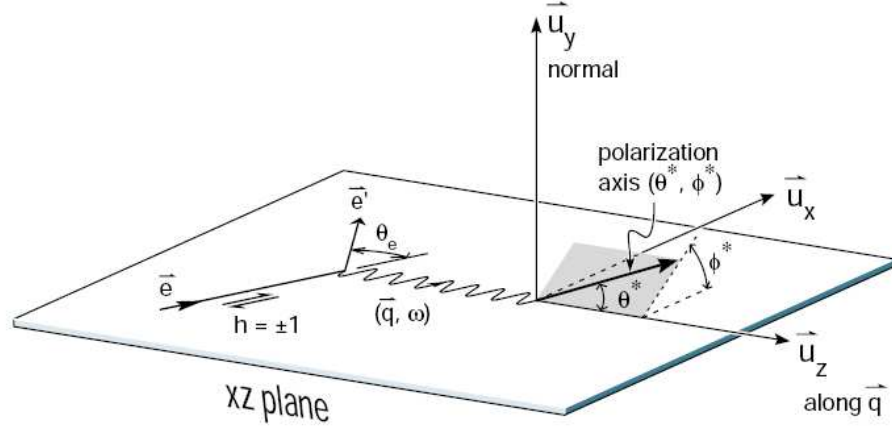


Fig. 10. Coordinate system for the reaction $\bar{p}(\vec{e}, e')p$.

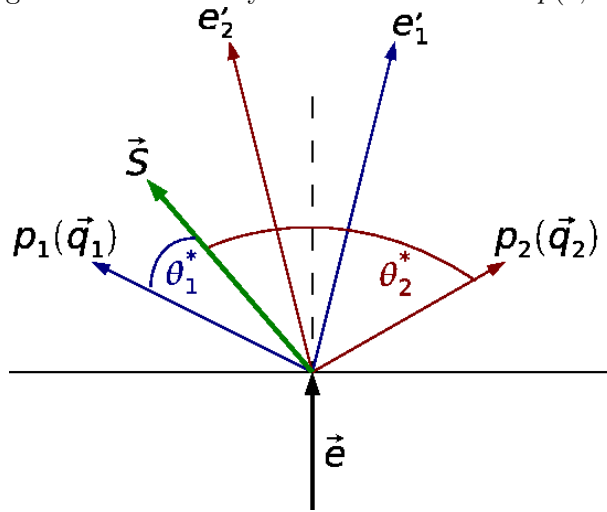


Fig. 11. The kinematics for the two simultaneous measurement. The scattered electrons e'_1 and e'_2 are detected in HRS_{Right} and HRS_{Left} respectively. The protons p_1 and p_2 recoil in the direction of the q -vectors \vec{q}_1 and \vec{q}_2 respectively. \vec{S} denotes the target spin polarization vector.

We may then invert the ratio of the asymmetries to obtain the equation

$$\mu_P \frac{G_E^P}{G_M^P} = -\mu_P \frac{a(\tau, \theta) \cos \theta_1^* - \frac{f_2}{f_1} \Gamma a(\tau, \theta) \cos \theta_2^*}{\cos \phi_1^* \sin \theta_1^* - \frac{f_2}{f_1} \Gamma \cos \phi_2^* \sin \theta_2^*} \quad (10)$$

Where $a(\tau, \theta) = \sqrt{\tau(1 + (1 + \tau) \tan^2(\theta_e/2))}$, $\theta_i^*(\phi_i^*)$ are the polar (azimuthal) angle of the target spin with respect to the \vec{q} in the i^{th} spectrometer, and $\Gamma = \frac{A_1}{A_2}$ is the ratio of the asymmetries between the two spectrometers (note that P_b , P_t and f cancel out when taking the ratio).

Polarized Target

For the part II of the experiment we plan to use the solid polarized proton target developed by UVa. In this target the material is $^{15}\text{NH}_3$ which is polarized by Dynamic Nuclear Polarization (DNP) [56] in a low temperature ($\approx 1^\circ\text{K}$) high magnetic field (5T). The target is irradiated with 140 GHz microwave radiation which drives the hyperfine transitions that align the nucleon spins. This target was used in various SLAC experiments as well as JLAB experiments such as SANE [57], E-93-026 [58], and RSS [59]. The proton polarization can reach as high as 95% and will decrease due to radiation damage, so that an average polarization of 75% may be achieved.

The target consists of superconducting Helmholtz coils which operate at 5 Tesla, a ^4He evaporation refrigerator, a pumping system, a high power microwave tube and an NMR system for measuring the target polarization. Figure 12 shows a side view of the target.

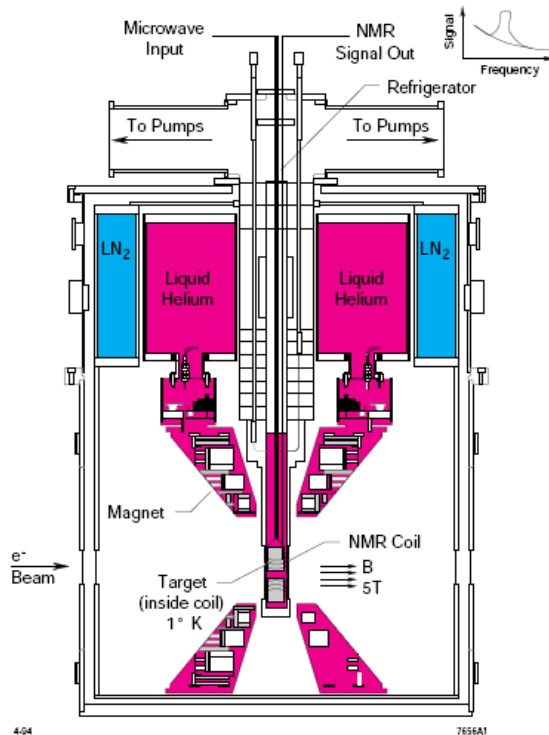


Fig. 12. Sideview of the UVa polarized target.

For this experiment the target spin will be aligned at 20° w.r.t. the beamline.

The target cell is filled with frozen ammonia granules and is fixed to a target holder stick and lowered into a cryostat of liquid ^4He . The nitrogen, helium and other target holder materials are in the acceptance of the HRSs and will dilute the measured asymmetry. The dilution factor will be addressed later. The unpaired proton in the ^{15}N can be polarized, hence a correction to the asymmetry must be made during the analysis, note however, that taking the ratio of the measured asymmetries greatly reduces the size of the necessary correction.

Radiation from the beam will gradually reduce the polarization of the target during the experiment. This can be partially recovered by target annealing, where the ammonia is warmed to $\approx 80\text{K}$. Eventually the target material must be changed, this must be done every 80 hours of $\approx 80\text{ nA}$ beam.

The strong magnetic field of the target will have an effect on the scattering of the electrons, but this may be corrected for using simulations. Since the two HRSs are at different angles with respect to the target magnetic field the correction will be different for each HRS. The uncertainty in the target spin direction is the leading systematic uncertainty in the extraction of the form factor ratio. During previous experiments it has been shown that the field direction is known to 0.1° [60].

Chicane

Since the polarization direction of the target will be held at 20° angle to the beam axis a non-negligible deflection of low energy electrons will be created. In order to ensure proper beam transport a set of chicane magnets will be added to the Hall A beam line. Since the (conditionally approved) δ_{LT} experiment [61] plans to use the same polarized target with the polarization direction held perpendicular to the beam axis, the deflection angle in this experiment will be ≈ 2.9 smaller than for that proposal. Thus, we propose to use the same beam line instrumentation being designed for the δ_{LT} experiment.

Septum Magnets

This proposal requires the installation of the two septum magnets in order to detect the scattered electrons at forward angles. Since we require measurements at several different angles, the septum magnets will not be vacuum coupled to the HRS to allow the HRSs to be moved in a relatively short time.

In order to provide a means to perform precision optical studies, particularly of the interaction of the target magnetic field with the magnetic fields of the septa we propose to fit the target with both solid carbon and solid tantalum disks which will allow accurate reconstruction of elastic scattering events from the solid disks in the HRS.

Background

Table 3 details the calculated background rate for the different kinematics.

Table 3

Calculated background rates for Part II of the Experiment.

Q^2 (GeV ²)	Full Focal-Plan Rate (kHz)	Rate at Elastic Peak (1 MeV wide in W) (Hz)	Signal-to-Noise Ratio @ Elastic Peak (true / background)
0.015	581.0	3899	0.49
0.030	103.0	1303	0.68
0.040	51.4	700	0.91
0.060	142.0	1409	0.28
0.080	67.4	651	0.43
0.100	37.5	344	0.60
0.150	12.2	102	1.12
0.200	17.3	115	0.78
0.250	8.7	53	0.94
0.300	4.7	27	1.30
0.350	2.8	16	1.56
0.400	1.7	9	2.11

The effect of the background will be to increase the statistical uncertainty of the ratio by a factor of $\sqrt{N_{signal} + N_{bck}N_{signal}} = \sqrt{1 + 1/SNR}$.

Expected Uncertainties

Experimental Systematics

We estimate the uncertainty in the beam polarization to be 1.5%, but this uncertainty cancels out when taking the ratio of asymmetries in the two HRSs. Other error sources include the target spin direction, beam energy $\Delta E/E = 1 \times 10^{-3}$, central momentum $\Delta E'/E = 1 \times 10^{-3}$, and central angle $\Delta\theta_e = 2$ mr. Note that the uncertainties assumed are very conservative and are expected to be smaller during the actual run. The largest systematic uncertainty in the proposed technique comes from the uncertainty in the target spin direction. Table 6 detailed the projected systematic uncertainties on R .

Beam Charge Asymmetry

Since the beam charge asymmetry affects the asymmetry measured in both HRSs in exactly the same manner, it is a common factor which will cancel out when taking the ratio of asymmetries. Thus, there is no effect from beam charge asymmetries on this measurement.

Target Polarization

Target polarization can be measured to 2.5% using NMR, however since we plan on taking the ratio of the asymmetries measured in the HRSs the target polarization cancels out and does not effect the calculation of the form factor ratio.

Target Dilution Factor

Both HRSs are identical and the measurement is performed at $\theta_e \approx 6^\circ - 12^\circ$ meaning both HRSs essentially see the target as a point target. Thus we expect the dilution factor to be essentially identical for both HRSs, up to a second order correction which we assume to be on the order of $\left(\frac{\Delta f_1/f_2}{f_1/f_2}\right) \approx 0.1\%$.

Nitrogen Asymmetry

Even though there are several materials present in the target only the nitrogen contributes to the asymmetry measurement. Although the nitrogen asymmetry is less well understood than the proton asymmetry we are able to reduce the uncertainty by taking the ratio of asymmetries.

In the shell model picture (for ^{15}N) the unpaired nucleon is the 7th proton which is in the $p_{1/2}$ shell. Thus we expect the nitrogen asymmetry to be dominated by the asymmetry of that single proton. The polarization of the unpaired proton is reduced from that of the free proton by several factors. First, according to the Equal Spin Temperature hypothesis (EST) the polarization of the nitrogen is only 1/6 that of the proton. Second, due to the possibilities in the combination of angular momentum in the nucleus, the proton spin is anti-parallel to the ^{15}N spin for 1/3 of the time. From these factors we can expect $A_N/A_p \approx 6\%$, where $A_N(A_p)$ is the nitrogen (proton) asymmetry. The effect of the nitrogen asymmetry is further reduced by the dilution factor, only some 30% of the events in the elastic peak are due to nitrogen, thus, at worst we expect $\approx 2\%$ contribution from the nitrogen to the single arm asymmetry.

By taking the ratio of asymmetries we get:

$$\Gamma = \frac{f_p^1 A_p^1 + f_N^1 A_N^1}{f_p^2 A_p^2 + f_N^2 A_N^2} \quad (11)$$

where $f_p^i(f_N^i)$ is the proton (nitrogen) dilution factor in the i th HRS. Since the dilution factors are approximately equal between the two HRSs we get:

$$\Gamma = \frac{A_p^1}{A_p^2} \cdot \frac{1 + \frac{f_N^1 A_N^1}{f_p^1 A_p^1}}{1 + \frac{f_N^2 A_N^2}{f_p^2 A_p^2}} \sim \frac{A_p^1}{A_p^2} \cdot \left[1 - \left(\frac{f_N}{f_p} \frac{A_N}{A_p} \right)^2 \right] \quad (12)$$

The uncertainties in the nitrogen contribution are due to the shell model approximation

(20%) and the nitrogen polarization (10%), so that $A_N/A_p \approx 0.060 \pm 0.013$. Assuming that only nitrogen and hydrogen are in the target we can get a worst case estimate of the ratio of nitrogen to proton dilution factors. We further assume a 5% uncertainty in this ratio due to the reduction in statistics for the measurement of the proton asymmetry. We find that for the worst case scenario the contribution of the nitrogen asymmetry to the uncertainty of the ratio of asymmetries is $\Delta\Gamma/\Gamma \approx 0.02\%$.

Kinematics and Time Request for Part II of the Experiment

The proposed kinematics for the DSA run period are shown in Table 4. We propose to use a 85nA beam and three separate beam energies. Rates were estimated using the fit from [11] for the proton form factors.

Table 4

Proposed Kinematics for Part II of the Experiment. HRS_{left} and HRS_{right} will each be set up to symmetrically detect electrons on opposite sides of the beamline, each at the $(\theta_{e'}, E_{e'})$ values specified. The associated recoiling proton angle θ_p is provided for reference.

Q^2 (GeV^2)	E_{beam} (GeV)	$\theta_{e'}$ (deg)	$E_{e'}$ (GeV)	θ_p (deg)	Rate (Hz)	Hours
0.015	1.1	6.406	1.092	83.069	1898	6
0.030	1.1	9.098	1.084	80.194	890	6
0.040	1.1	10.535	1.078	78.675	639	6
0.060	2.2	6.430	2.168	79.360	400	6
0.080	2.2	7.444	2.157	77.725	278	6
0.100	2.2	8.345	2.146	76.288	206	6
0.150	2.2	10.289	2.120	73.242	114	6
0.200	3.3	7.899	3.193	72.678	90	6
0.250	3.3	8.871	3.166	70.691	50	6
0.300	3.3	9.761	3.140	68.909	35	12
0.350	3.3	10.590	3.113	67.284	25	12
0.400	3.3	11.372	3.086	65.783	19	12

Table 5 lists the projected (stat.) uncertainties for the proposed data points (for 20° target field orientation).

Table 6 shows the projected systematic uncertainties for the part II of the experiment.

Additional time is needed for the following purposes:

- 11 angle changes require 11 day shifts totaling 88 hours.
- 7 Target anneals require 1.5 hours each totaling 12 hours.
- 1 Target cell change requires 1 shift totaling 8 hours.
- 3 beam energy changes during the experiment, requiring about 24 hours.
- 12 pointing runs will be taken, totaling about 12 hours.
- 3 Møller measurements of the beam polarization are needed, requiring about 12 hours.

Table 5

Projected asymmetries for both HRSs and statistical uncertainties for part II of the experiment.

Q^2 (GeV^2)	A_1 (%)	A_2 (%)	$(\frac{\Delta R}{R})_{stat.}$ (%)	$(\frac{\Delta R}{R})_{stat.-bck.}$ (%)
0.015	1.93	1.84	0.23	0.40
0.030	3.84	3.62	0.24	0.37
0.040	5.09	4.77	0.25	0.36
0.060	3.81	3.38	0.27	0.59
0.080	5.03	4.40	0.29	0.53
0.100	6.25	5.38	0.30	0.49
0.150	9.19	7.69	0.35	0.48
0.200	7.95	6.36	0.36	0.54
0.250	9.73	7.64	0.44	0.63
0.300	11.44	8.85	0.35	0.46
0.350	13.09	10.01	0.40	0.51
0.400	14.69	11.12	0.44	0.53

- A systematic study of the spectrometer optics using the septum magnets and their interaction with the target magnetic field is needed. We are planning one day (12 hours) of measurements in order to perform a high precision study.
- Note: The angle and energy changes will be minimized while still covering the proposed kinematics.

Thus, our total time request for the DSA part is for 260 hours = 11 days.

Kinematic and Time Request Summary

We propose to perform two sets of measurement, using DSA for the very low Q^2 region and recoil polarization for the low Q^2 region. These measurements will be taken during separate run periods to accommodate lab constraints. The proposed kinematics are chosen to minimize the overall uncertainty in each of the data points and to have an overlap region where the two **different** techniques may be compared, possibly further reducing the systematic errors and testing the validity of the techniques used.

Figure 13 shows the proposed kinematics for both parts of the experiment and the projected total errors on the ratio.

Our total time request is:

- 14 days for the recoil polarimetry part (**conditionally approved by PAC31** - See Appendix B).
- 11 days for the DSA part.
- **Total time request 25 days.**

Table 6

Projected Systematic Uncertainties (%) on R for Part II of the Experiment.

Q^2 (GeV^2)	$\Delta E/E = 10^{-3}$	$\Delta\theta_e = 2mrad$	$\Delta\theta_{pol} = 0.1^\circ$	$\Delta\phi_{pol} = 0.1^\circ$
0.015	$2.55 \cdot 10^{-3}$	$1.14 \cdot 10^{-2}$	0.22	-
0.030	$3.65 \cdot 10^{-3}$	$1.62 \cdot 10^{-2}$	0.31	-
0.040	$4.24 \cdot 10^{-3}$	$1.88 \cdot 10^{-2}$	1.40	-
0.060	$1.31 \cdot 10^{-3}$	$1.16 \cdot 10^{-2}$	0.43	-
0.080	$1.53 \cdot 10^{-3}$	$1.35 \cdot 10^{-2}$	0.72	-
0.100	$1.74 \cdot 10^{-3}$	$1.52 \cdot 10^{-2}$	0.32	-
0.150	$2.20 \cdot 10^{-3}$	$1.89 \cdot 10^{-2}$	0.29	-
0.200	$1.15 \cdot 10^{-3}$	$1.48 \cdot 10^{-2}$	0.35	-
0.250	$1.33 \cdot 10^{-3}$	$1.68 \cdot 10^{-2}$	0.34	-
0.300	$1.50 \cdot 10^{-3}$	$1.87 \cdot 10^{-2}$	0.35	-
0.350	$1.66 \cdot 10^{-3}$	$2.06 \cdot 10^{-2}$	0.35	-
0.400	$1.83 \cdot 10^{-3}$	$2.23 \cdot 10^{-2}$	0.35	-

Q^2 (GeV^2)	$(\Delta(f_1/f_2))/(f_1/f_2) = 0.1\%$	$A_N/A_p = 0.06 \pm 0.013$	Total
0.015	0.770	0.043	0.80
0.030	0.562	0.080	0.65
0.040	0.495	0.093	1.42
0.060	0.410	0.197	0.63
0.080	0.367	0.208	0.83
0.100	0.330	0.216	0.51
0.150	0.290	0.231	0.47
0.200	0.260	0.277	0.52
0.250	0.252	0.288	0.51
0.300	0.243	0.298	0.52
0.350	0.238	0.308	0.52
0.400	0.235	0.316	0.53

Note that should both parts be approved, we plan to forgo the lowest Q^2 point for the polarization ratio part, bringing the total time request down to 23 days. Further note that this does not include setup time for the polarized target and septum magnets in Hall A.

Note that since the first part of the experiment was conditionally approved by PAC31, we are requesting an incremental increase in the approved beam time of 9-11 days which will extend our approved measurements a **factor of 20 lower in Q^2 .**

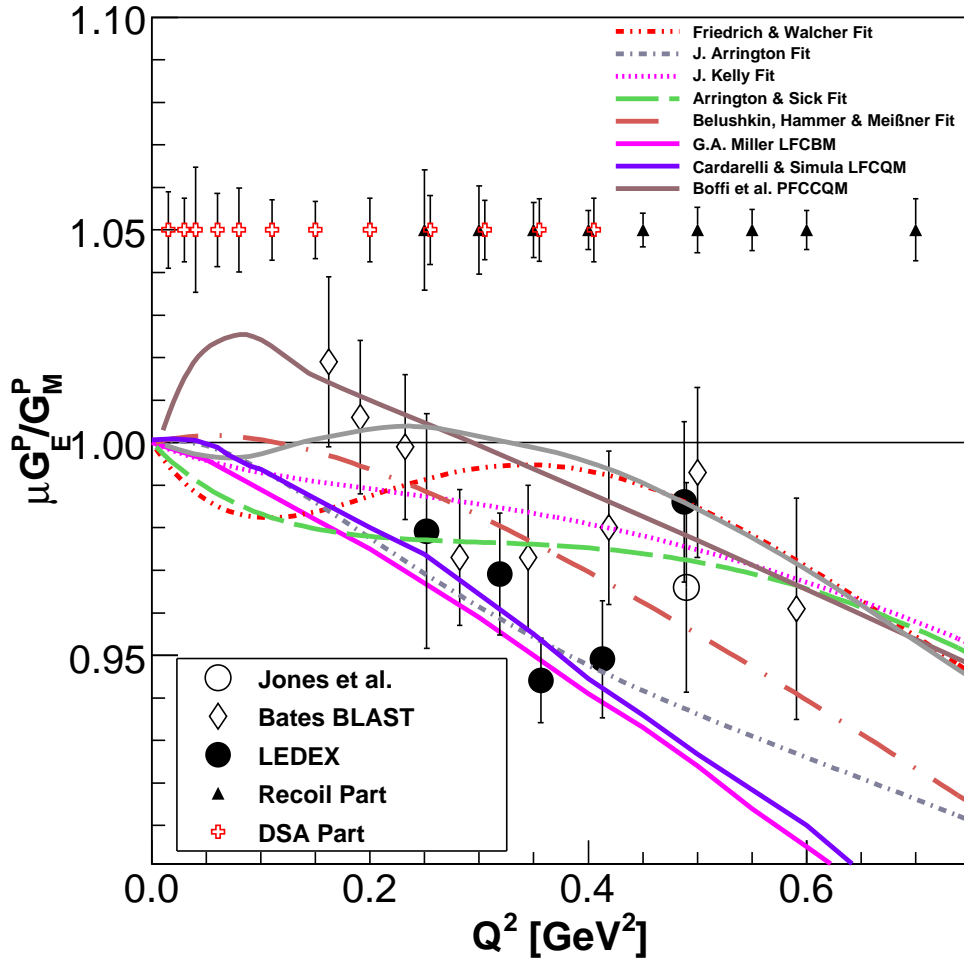


Fig. 13. Proposed kinematics and projected total uncertainties (stat.+syst.).

Collaboration, Conflicting Experiments and Scheduling

The core of the current collaboration consists of individuals who have been deeply involved in previous Hall A polarization experiments and polarized target experiments.

In order to run part II of this experiment a polarized target must be installed in Hall A, a major installation, thus it is proposed to schedule this experiment in tandem with other polarized target experiments planned for Hall A [61].

A PAC Report on PR-01-105

Proposal: PR-01-105

Title: G_{Ep} / G_{Mp} via Simultaneous Asymmetry Measurements of the Reaction $\vec{p}(\vec{e}, e')$

Spokesperson: G. Warren

Motivation: The ratio G_{Ep} / G_{Mp} is vital to our understanding of the structure of the proton. Results from Hall A experiments using electron-proton polarization transfer have shown that this ratio clearly decreases with increasing Q^2 . An experiment based on the Rosenbluth separation method (E-01-001) has been approved to check on these findings. The proposed experiment aims at providing another check with different systematic uncertainties and high statistical precision.

Measurement and Feasibility: The polarized beam polarized target asymmetry is to be measured simultaneously, using two spectrometers at the same Q^2 , for different orientations of the proton polarization. The ratio of both cross sections is a function of G_{Ep} / G_{Mp} . In this ratio the degrees of polarization and the dilution factor of the target drop out to first order, thus minimizing systematic uncertainties. It is proposed to measure G_{Ep} / G_{Mp} at $Q^2=1.1$ and 2.1 (GeV/c)².

Issues: The proposal is clearly written and the underlying idea is very good. However, given the existing data and the approved experiment to check on them, the PAC does not find a compelling reason to approve this proposal at the present time.

Recommendation: Defer

Scientific Rating: N/A

B PAC Report on PR-07-004

Proposal: PR-07-004

Scientific Rating:

Title: Measurement of the Proton Elastic Form Factor Ratio at low Q^2

Spokespersons: R. Gilman, D.W. Higinbotham, G. Ron

Motivation:

The aim is the precision measurement of the proton elastic form-factor ratio $\mu G_E / G_M$ in the range of $Q^2 = 0.25 - 0.7 \text{ GeV}^2$. A point-to-point systematic uncertainty of better than 1% is sufficient to map out any changes in shape of the ratio in this Q^2 region. The measurement will use the recoil polarization method which determines the form-factor ratio more directly than the Rosenbluth separation. An important by-product of precise knowledge of the electric to magnetic ratio is that, when combined with other high statistics measurements of the cross-sections, this will reduce uncertainties in the Zemach radius, which is the key parameter in fixing the hyperfine corrections to the Hydrogen atom. The ratio of form-factors is a fundamental measurement. Determination of the precise Q^2 dependence will eliminate speculative parametrizations and motivate further theoretical work.

Measurement and Feasibility:

The group has shown with the limited LEDEX running that this experiment is feasible to the precision proposed.

Issues:

Since Mainz is presently running an experiment which using Rosenbluth separation can determine the same ratio in the same region of Q^2 , consideration should be given to these results and especially their level of uncertainties before approval to proceed with this proposal is given.

Recommendation: C2=Conditionally Approve w/PAC Review

References

- [1] M.N. Rosenbluth. Phys. Rev. **79**, 615 (1950).
- [2] W. Bartel *et al.*, Phys. Lett. **33B**, 245 (1970).
- [3] C. Berger *et al.*, Phys. Lett. **35B**, 87 (1971).
- [4] R.G. Arnold *et al.*, Phys. Rev. Lett. **57**, 174 (1986).
- [5] L. Andivahis *et al.*, Phys. Rev. D **50**, 5491 (1994).
- [6] M.E. Christy *et al.*, Phys. Rev. C **70**, 015206 (2004).
- [7] I. Qattan *et al.*, Phys. Rev. Lett. **94**, 142301 (2005).
- [8] F. Borkowski *et al.*, Nucl. Phys. **A222**, 269 (1974).
- [9] F. Borkowski *et al.*, Nucl. Phys. **B93**, 461 (1975).
- [10] G.G. Simon *et al.*, Nucl. Phys. **A333**, 381 (1975).
- [11] J. Arrington, Phys. Rev. C **69**, 022201 (2004).
- [12] M. Jones *et al.*, Phys. Rev. Lett. **84**, 1398, (2000).
- [13] O. Gayou *et al.*, Phys. Rev. C **64**, 038202, (2001).
- [14] O. Gayou *et al.*, Phys. Rev. Lett. **88**, 092301 (2002).
- [15] F. Iachello, A. D. Jackson and A. Lande, PLB **43**, 191 (1973).
- [16] G. Hohler *et al.*, NPB **114**, 505 (1976).
- [17] M. Gari and W. Krupelmann, Z. Phys **A322**, 689 (1985).
- [18] P. Mergell, U. G. Meissner and D. Dreschel, Nucl. Phys. A **596**, 367 (1996).
- [19] E. L. Lomon, Phys. Rev. C **64**, 035204 (2001).
- [20] H. W. Hammer and U. G. Meissner, Eur. Phys. J. A **20**, 469 (2004).
- [21] F. Iachello and Q. Wan, Phys. Rev. C **69**, 055204 (2004).
- [22] R. Bijker and F. Iachello, Phys. Rev. C **69**, 068201 (2004).
- [23] M. A. Belushkin, H. W. Hammer and U. G. Meissner, Phys. Rev. C **75**, 035202 (2007).
- [24] F. Cardarelli *et al.*, Phys. Rev. C **62**, 065201 (2000).
- [25] D. H. Lu, A. W. Thomas and A. G. Williams, Phys. Rev. C **57**, 2628 (1998).
- [26] G. A. Miller, Phys. Rev. C **66**, 032201(R) (2002).
- [27] S. Boffi *et al.*, Eur. Phys. J. A **14**, 17 (2002).
- [28] A. Faessler *et al.*, Phys. Rev. D **73**, 114021 (2006).

- [29] S. Simula, Proceedings of the Int'l Conf. on "The Physics of Excited Nucleons" (N* 2001).
- [30] A.I. Akhiezer and M.P. Rekalov, Sov. Phys. Doklady **13**, 572 (1968).
- [31] N. Dombey, Rev. Mod. Phys. **41**, 236 (1969).
- [32] A.I. Akhiezer and M.P. Rekalov, Sov. J. Part. Nucl. **3**, 277 (1974).
- [33] Th. Pospischil *et al.*, Eur. Phys. J. A **12**, 125 (2001).
- [34] V. Punjabi *et al.*, Phys. Rev. C **71**, 055202 (2005).
- [35] A. Afanasev, I. Akushevich, and N.P. Merenkov, hep-ph/0208260.
- [36] P.A.M. Guichon and M. Vanderhaeghen, Phys. Rev. Lett. **91**, 142303 (2003)
- [37] P.G. Blunden, W. Melnitchouk, and J.A. Tjon, Phys. Rev. Lett. **91**, 142304 (2003).
- [38] Y.C. Chen *et al.*, Phys. Rev. Lett. **93**, 122301 (2004).
- [39] A. Afanasev *et al.*, Phys. Rev. D **72**, 013008 (2005).
- [40] S.P. Wells *et al.*, Phys. Rev. C **63**, 064001 (2001).
- [41] F.E. Maas *et al.*, Phys. Rev. Lett. **94**, 082001 (2005).
- [42] G. Ron *et al.*, Phys. Rev. Lett. **99**, 202002 (2007).
- [43] G. Warren *et al.* Jefferson Lab Proposal PR-01-105.
- [44] J. Friedrich and Th. Walcher, Eur. Phys. J. A **17**, 607 (2003).
- [45] M. R. Frank, B. K. Jennings and G. A. Miller, Phys. Rev. C **54**, 920 (1996).
- [46] S. Simula, Private Communication.
- [47] P. Achenbach *et al.*, Mainz A1 Collaboration.
- [48] G. A. Miller, E. Piassetzky and G. Ron, To be submitted to PRL.
- [49] See V. Nazaryan, C.E. Carlson, and K.A. Griffioen, Phys. Rev. Lett. **96**, 163001 (2006) and references therein.
- [50] K. Aniol *et al.*, Phys. Rev. C **69**, 065501 (2004).
- [51] K. Paschke *et al.*, Jefferson Lab Experiment E05-109.
- [52] R. Gilman *et al.*, E05-103, Low Energy Deuteron Photodisintegration (<http://hallaweb.jlab.org/experiment/LEDEX/documents/PR05-103.pdf>).
- [53] D. Higinbotham *et al.*, E05-004, A(Q) at low Q in ed Elastic Scattering (<http://hallaweb.jlab.org/experiment/LEDEX/documents/PR05-004.pdf>).
- [54] M. W. McNaughton *et al.*, Nucl. Inst. Meth. A **241**, 435-440 (1985).
- [55] G. Ron *et al.* To be submitted to NIM.
- [56] W. de Boer, J. Low Temp. Phys. **22**, 185 (1976).

- [57] O. Rondon-Aramayo *et al.*, Jefferson Lab Proposal E-07-003.
- [58] D. Day *et al.*, Jefferson Lab Experiment E-93-026.
- [59] O. Rondon-Aramayo *et al.*, Jefferson Lab Experiment E-01-006.
- [60] D. Day, Private Communication.
- [61] K. Slifer *et al.* Jefferson Lab Proposal PR-07-001.